Desalination and Water Treatment
www.deswater.com
doi: 10.1080/19443994.2014.981415

56 (2015) 2576–2583
December

Taylor & Francis
Taylor & Francis Group

Experimental study of the inclined solar film evaporator

S. Saidi[a,d,*], R. Ben Radhia[a,b], B. Dhifaoui[a,c], S. Ben Jabrallah[a,d]

[a]*Laboratory of Energy, Heat and mass Transfer, Campus University, Tunis 1060, Tunisia, Tel. +216 25 832 801; email: sirine274@live.fr (S. Saidi), Tel. +216 50 426 697; email: rymo2001@yahoo.fr (R. Ben Radhia), Tel. +216 97 753 051; email: dhifaouib@gmail.com (B. Dhifaoui), Tel. +216 98 486 708; Fax: +216 72 590 566; email: sadok.jabrallah@fsb.rnu.tn (S. Ben Jabrallah)*
[b]*Faculty of Sciences of Gafsa, Campus University, Gafsa 2112, Tunisia*
[c]*Higher Institute of Applied Science and Technology, Mateur, Tunisia*
[d]*Faculty of Sciences of Bizerte, University of Carthage, Bizerte 7021, Tunisia*

Received 10 December 2013; Accepted 11 August 2014

ABSTRACT

The present study investigated the experimentation of an inclined solar film evaporator in the meteorological conditions of the town of Bizerte, in Tunisia. The experimental device used in this study has a parallelepiped form. It is primarily constituted by an inclined metal plane plate. A water film falls on the external face of this plate through a porous tissue. A glass cover, placed on a wooden frame put on the plate, is exposed to the solar radiation acting as a solar panel. An ascending air flow enters in the evaporator where it is in direct contact with the falling water film. This experimental device is designed and supplemented by a protocol of measurements to conduct this study. The thermocouples installed along the metal plate were connected to an automatic acquisition making it possible to read and store the measured temperatures values. The evaporated flow is measured by an electronic balance and a stopwatch. The humidity and the air velocities are measured using a digital multifunction device. The series of measurement are carried out in natural and forced convections. The profile of the liquid film temperature and the variation of the evaporated flow are measured for the two convection modes. To quantify the effectiveness of the solar evaporator, the thermal and mass yields are calculated. The results show that the evaporated flow is more significant in forced convection and that the thermal and mass yields of the solar evaporator are higher than 80%.

Keywords: Solar evaporator; Liquid film; Natural convection; Forced convection; Yield

1. Introduction

The water requirements in the world increase in a continuous manner, whereas the underground reserves are decreasing constantly. One of the solutions that can contribute to the increase of the potentialities in water is the desalination of the sea water or the brackish waters. Indeed, the solar distillation is a solution adapted to provide the fresh water because it uses a gratis energy source. It appeared in

*Corresponding author.

Presented at the 4th Maghreb Conference on Desalination and Water Treatment (CMTDE 2013)
15–18 December 2013, Hammamet, Tunisia

1872 close to Las Salinas in the north of the Chili [1]. The solar still knew several modifications to improve its yield. Tiwari et al. [2] used a solar still in double slope. The authors showed that the used device has a best yield in the climatic conditions of summer, and that in winter the simple slope distiller has a more elevated yield than the double slope distiller. Rajvanshi [3] put a soluble black stain water to increase the absorption. It obtained an increase in 29% yield compared with the solar still for conventional greenhouse effect. Bouchekima et al. [4] studied numerically and experimentally a capillary film still. The experimental tests are achieved in Touggourt in the south of Algeria. In these experiences, the ambient temperature is close to 40°C and the water supply is geothermal. The numerical results show that the maximum mass flow rate distillate is about 1.3 $L/h/m^2$ and it is obtained at 12 o'clock. Al-Garni [5] carried out a numerical and experimental study on a greenhouse effect solar still with only one slope, while using a water heater and a ventilator to cool the surface outside of the glazing. The experimental results showed that the productivity of the system increases until 250% when a heating of about 500 W is applied to water in the still and an external cooling ventilator is used. An increase in the productivity from 5.2 to 10.3% is observed for wind velocities which vary from 7 to 9 m/s. The author also noted that a good concordance exists between the experimental and numerical results. Sethi et al. [6] investigated an experimental study on a greenhouse effect solar still with double slope in the forced convection. The results show that the daily thermal efficiency of the solar still increases from 13.55 to 31.07%.

In spite of the improvements brought to the conventional solar stills, the yield is weak because the evaporation and the condensation take place in the same enclosure. Indeed, the competition between the two antagonistic phenomena from the energy point of view is opposed to the improvement of the distilled water production. The separation of these two phenomena seems to bring a solution to weak yield of the solar stills. Orfi et al. [7] studied a solar desalination system that contains two solar panels of air and water, a humidifier and a condenser. The experimental study consists of measuring the temperatures and the humilities at the inlet and the exit of the different components of the desalination system. The conducted theoretical study consists of posing a mathematical model to describe the heat and mass transfers in the evaporator and the condenser. The theoretical results show that there exists a report between the optimal mass flow at the inlet of the corresponding condenser and the maximal production of fresh water. Marmouch et al. [8] carried out a theoretical study to test the effect of a cooling tower on the production of a solar desalination system that contains an evaporator, a condenser, two solar panels of air and of water, and a tower of cooling. A mathematical model based on the mass and the energy conservation equations is developed to conduct this study. The results show that this desalination unit can produce fresh water with high rates exceeding 37 $L/d/m^2$ when using the cooling tower, whereas the production of the system is 15 $L/d/m^2$ without the cooling tower. El-Shazlya [9] et al. studied experimentally a solar desalination system by humidification–dehumidification that contains a solar collector, a condenser and an evaporator. The authors studied the influence of the inclination angle of the solar collector, the effect of the feed water flow rate in the evaporator, and the effect of recycling of the hot brine. The results show that the efficiency of the solar collector increases by increasing the inclination angle until 45°. It shows also that the desalination unit productivity increased by increasing of the feed water flow rate to attain 5 L/min and then decreases beyond this value. The unit productivity also increases by the recycling of the hot brine.

Several studies were carried on the liquid films evaporation due to their wide application in several domains. These liquid films of very weak thickness have the advantage to intervene high exchanges coefficients. According to the manner in which the phenomenon of evaporation is achieved, several cases can be mentioned in this context. Since the motor of evaporation is heating, this last can be applied directly to the wall (by a heat flux density) where the film is falling [10–16] or by an imposed temperature [17]. This heating can also be applied to the air flow in contact with the liquid film [18,19] or to the liquid film flow [20].

This work consists of an experimental study on the evaporation of a water–liquid film flowing on an inclined solar evaporator in view of the production of fresh water. This film falls on the external surface of an inclined plane plate through a porous tissue. An ascending air flow is in direct contact with the water film. The experimental study was carried on real site allowing to characterize the solar evaporator performance and to compare this yield with the two types of convection.

2. Materials and methods

2.1. Experimental device

To carry out this study, an experimental device (Fig. 1) was designed. The solar evaporator has parallelepiped shape length $L = 2$ m, width $b = 1$ m, and height $h = 0.22$ m. It is composed of primarily by a

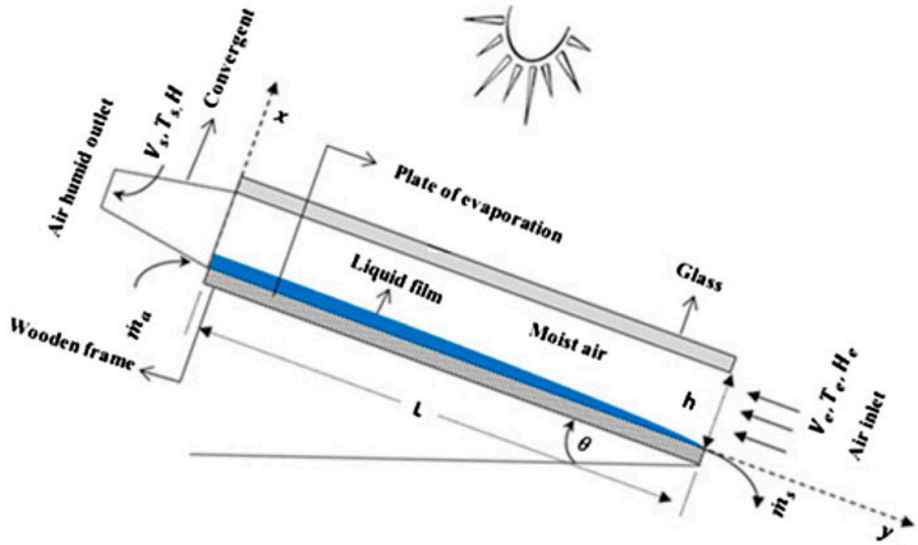

Fig. 1. Experimental device and problem position.

metal flat plate which plays the role of the absorber, a glass cover exposed to solar radiation playing the role of solar panel, a wooden frame which back insulated by glass wool, and a metallic structure that maintains all the components. The water supply in the humidifier is provided by a constant level reservoir which is connected to a copper tube disposed above the absorbing plate. This tube was perforated with holes of small diameter allowing the passage of water on the plate to form the falling liquid film. A valve is placed at the inlet of the evaporator to fix the feed water flow rate. To recover the brine, a plastic tube is placed above the evaporator. To avoid dry areas and uniformly wet the plate, porous fabric is pasted on it to support the liquid film. The humidifier is placed on a stand making an angle $\theta = 35^\circ$ which is horizontal to receive the maximum of solar energy.

The solar evaporator functioning is explained by: the air flow ascending enters the evaporator where it is in direct contact with the falling water film. This air humidifies itself following the evaporation of the film submitted to the solar radiation. Then this air goes to the condenser where steam in condensed is a second step for recovering fresh water.

2.2. Measuring device

The solar evaporator is supplemented by a measurement system. Ten K-type thermocouples (Chromel/Alumel) are placed along the porous fabric covering the evaporation plate to measure the temperature of the falling liquid film. The thermocouples connect to an automatic acquisition unit which allowing reading and storing during the time the measured temperature values. The moistures and air velocities at the inlet and the outlet of the air in the evaporator are measured using a multifunction device digital Testo 445. An electronic balance and a stopwatch are used to measure the flow rates of feed water and the brine.

In fact, in the absence of evaporation, the mass flow rate of feed water merges with the mass flow of the brine so that:

$$\dot{m}_a = \frac{\mathrm{d}m_s}{\mathrm{d}t} \tag{1}$$

In the absence of evaporation, the feed flow rate merges with the flow rate of the brine. The evaporated flow rate is calculated by the difference between the feed water flow rate and the brine flow rate so that:

$$\dot{m}_{\mathrm{evp}} = \dot{m}_a - \dot{m}_s \tag{2}$$

A meteorological station is installed to record the solar flow. A diffuser placed at the top of the evaporator which connected to the blower allows the aspiration of the air for the forced convection.

Temperatures are measured in this study using K-type thermocouples with an uncertainty $\Delta T = 0.5$°C. The velocity and humidity of the air are measured with uncertainty $\Delta V = 0.05\ \mathrm{ms}^{-1}$ and $\Delta H = 0.2\%$. The liquid flow rate is calculated by $\dot{m} = m/t$, where m is the mass of liquid collected during the time period of t. Mass is measured using an electronic balance with a sensitivity $\Delta m = 0.1$ g. Time uncertainty is 0.3 s so that $\Delta\dot{m}/\dot{m} = 0.03\%$.

Fig. 2 represents two photographs of the experimental device on real site equipped by the measurement system.

3. Results and discussion

3.1. Distribution of the temperature along the liquid film

In order to better understand the phenomenon of evaporation, particular attention is given to the liquid film temperature since it allows describing of the evaporator behavior. Fig. 3 represents the evolution of the liquid film temperature along the plate of evaporation during the day of 12 June 2013 in natural convection. The evolution of this parameter is characterized by the existence of two zones. The first zone is located at the top of the evaporator between $y = 0$ and $y = 0.4$ m where is an elevation of the liquid film temperature. Therefore, this area is a heating zone (sensitive heat). The second area covers the rest of the surface of the plate of evaporation. The film temperature decreases along this surface. In fact, the heat supplied by the solar radiation is transformed into latent heat. Therefore, this area is an evaporation zone. The presence of these two areas has been highlighted by Ben Jabrallah et al. [11], while studying the water film evaporation falling on a wall heated by a constant flux density in a rectangular cavity.

The existence of these two zones is also justified for the forced convection under operating parameters of Bizerte region (Fig. 4). Indeed, when aspiring air the profile of the temperature of the liquid film along the evaporator undergoes an increase then a reduction. It must be noticed that in forced convection, the liquid film temperature profiles present a lower maximum than these in natural convection. It can be explained by the aspiration of air that is at the origin of the liquid flow cooling on the one hand, and on the other hand, by the intensification of the evaporation in the forced convection case. The maximum of the temperature is obtained toward 14 h for the two types of convection.

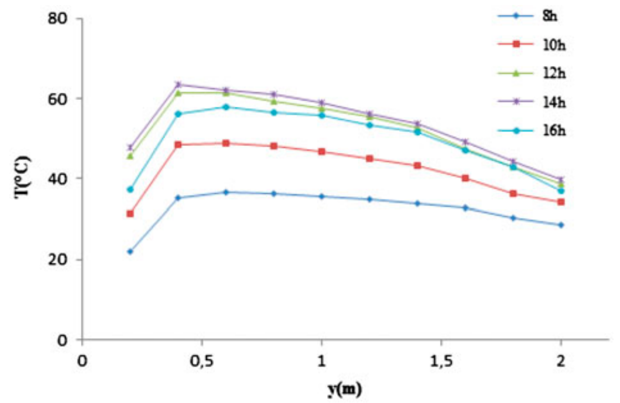

Fig. 3. Distribution of the liquid film temperature along the evaporator in natural convection (NC) during the day of 12 June 2013 ($G_{moy} = 766.1$ W m^{-2}, $T_{amb} = 32$°C, $H_{amb} = 49\%$, and $\dot{m}_a = 4.1$ kg h^{-1}).

3.2. Variation of the liquid film temperature during the day

Fig. 5 represents the variation of the liquid film temperature during the day for different positions y of

Fig. 2. Solar evaporator on real site.

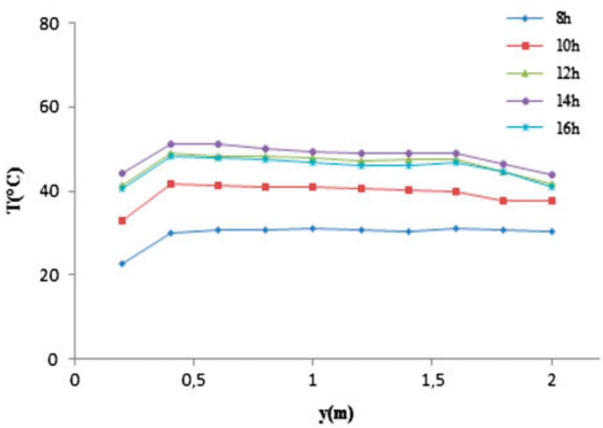

Fig. 4. Distribution of the liquid film temperature along the evaporator in forced convection (FC) during the day of 07 July 2013 (G_{moy} = 770.7 W m^{-2}, T_{amb} = 34°C, H_{amb} = 46%, $\dot{m}_a$ = 4.1 kg h^{-1}, and V = 4.05 ms^{-1}).

the evaporation plate and the variation of the solar flux density in natural convection. The profile of the solar flux density and the liquid film temperatures takes almost the same shape. In fact, this profile is characterized by the existence of two periods. In the first period, the temperature increases until about 12 h. The second period that extends for the remaining of the day is characterized by the reduction of the liquid film temperature following the decrease in solar radiation in the afternoon. It is to notice that the temperature profile is higher for the position y = 0.4 m in conformity with Figs. 3 and 4.

Fig. 6 confirms the result of the forced convection mode where the liquid film temperature profiles follow the solar flux density profile during the day, because the solar radiation is the essence of the evaporation. The liquid film temperature profiles during the day show that the maxima of temperatures are lower in the case of forced convection than those in the case of natural convection.

3.3. Variation of the evaporated mass flow rate during the day

To better explain the performance of the solar evaporator, the evaporated mass flow rate and of the solar flux density evolutions, during the days of 14 June 2013 and 04 July 2013 in natural and forced convection, are given in Fig. 7. In fact, the profiles of the evaporated mass flow rate have the same paces that those of the solar flux density. The maxima of the solar flux density are reached at 13 h whereas the maxima of the evaporated mass flow rate are reached at 14 h. This shift of one hour in the level of the maxima can be explained by the thermal inertia of the system. While aspirating air, the maximum gap between the two profiles of the evaporated mass flow rate in natural and in forced convection is 43% although the average solar flux density of the two types of convection is very close. Therefore, the evaporation process is improved by the air aspiration. The evaporated mass flow rate accumulated during the day for the two types of convection inform us about the production of the solar evaporator is calculated. This production is more than 21 L/d in the case of the forced convection which shows a production improvement of 7 L in relation to the natural convection. This

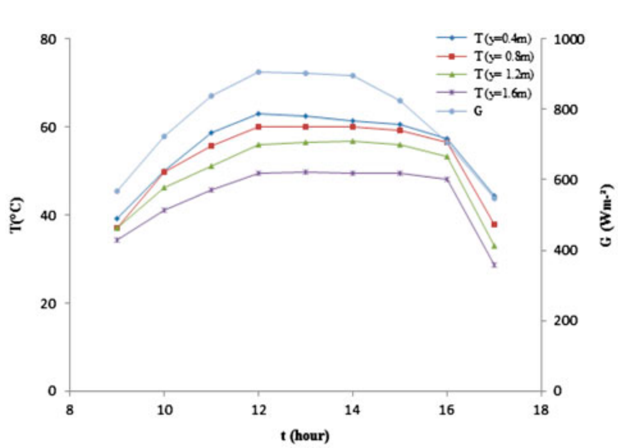

Fig. 5. Evolution of the temperature of the liquid film and solar flow in natural convection (NC) during the day in natural convection of 12 June 2013 (G_{moy} = 766.1 W m^{-2}, T_{amb} = 32°C, H_{amb} = 49%, and $\dot{m}_a$ = 4.1 kg h^{-1}).

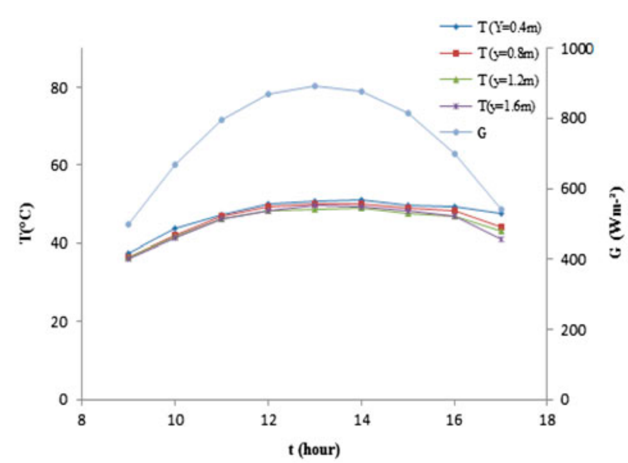

Fig. 6. Evolution of the liquid film temperature and solar flow in forced convection (FC) during the day of 07 July 2013 (G_{moy} = 770.7 W m^{-2}, T_{amb} = 34°C, H_{amb} = 46%, $\dot{m}_a$ = 4.1 kg h^{-1}, and V = 4.05 ms^{-1}).

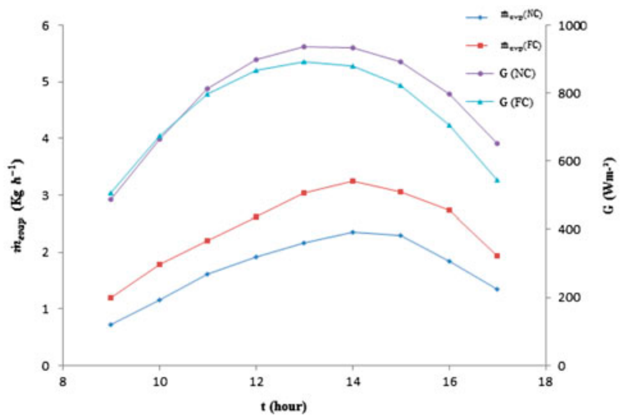

Fig. 7. Evolution of the evaporated flow rate and of the solar flow during the day in natural and forced convection. (NC): (14 June 2013) $G_{\text{moy}} = 785.1$ W m^{-2}, $T_{\text{amb}} = 31$°C, $H_{\text{amb}} = 51\%$, $\dot{m}_a = 4.1$ kg h^{-1}. (FC): (04 July 2013) $G_{\text{moy}} = 784.1$ W m^{-2}, $T_{\text{amb}} = 32$°C, $H_{\text{amb}} = 48\%$, and $G_{\text{moy}} = 4.1$ kg h^{-1}, $V = 3.34$ ms^{-1}.

result highlights the importance of working in forced convection in order to enhance the evaporator production. The same result was obtained by Wang et al. [21].

3.4. Variation of the thermal yield during the day

To estimate the efficiency of the solar evaporator, the thermal and mass yields are calculated. The thermal yield is defined as the ratio between the heat flux used by the evaporation i.e. latent heat flux and the heat flux radiated by the sun. So, the thermal yield expresses as [22]:

$$\eta = \frac{\dot{m}_{evp} L_v}{GS} \tag{3}$$

The evolution of the thermal yields and solar flux density during the day in natural and forced convection is shown in Fig. 8. This parameter varies in the same way as that of the solar flux density. It increases in the morning as far as reaching a maximum at about 14 h, and then it decreases for the rest of the day. The thermal yield of the system is improved by 26% in the case of the forced convection in relation to the natural convection. In fact, the maximum thermal yield increases from 0.69 in the case of the natural convection to 0.9 in the case of the forced convection. This result is demonstrated in the literature by Cherif et al. [14].

3.5. Variation of the mass yield during the day

The mass yield of the solar evaporator is defined as being the ratio of the evaporated mass flow rate by the mass flow rate of feed water [14]:

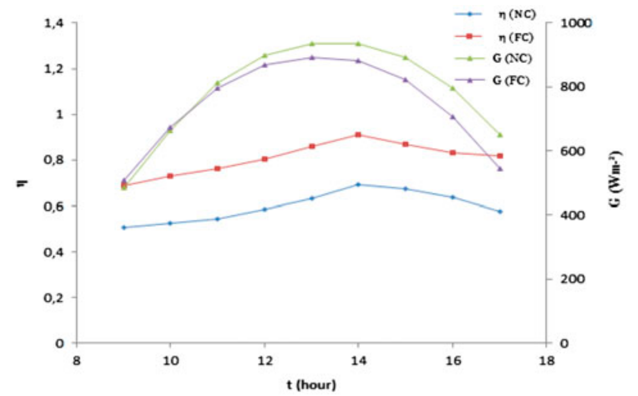

Fig. 8. Evolution of the thermal yield and the solar flow during the day in natural and forced convection. (NC): (14 July 2013) $G_{\text{moy}} = 785.1$ W m^{-2}, $T_{\text{amb}} = 31$°C, $H_{\text{amb}} = 51\%$, $\dot{m}_a = 4.1$ kg h^{-1}. (FC): (04/07/2013) $G_{\text{moy}} = 784.1$ W m^{-2}, $T_{\text{amb}} = 32$°C, $H_{\text{amb}} = 48\%$, and $\dot{m}_a = 4.1$ kg h^{-1}, $V = 3.34$ ms^{-1}.

$$\tau = \frac{\dot{m}_{evp}}{\dot{m}_a} \tag{4}$$

The variation of the mass yields and solar flow during the day in natural and forced convection is illustrated in Fig. 9. It appears that the mass yield varies in the same way as that of the solar flux density. It increases in the morning period as far as reaching a maximum at about 14 h and then it decreases for the rest of the day. Since, the maximum mass yield increases from 0.57 in the natural convection case to 0.79 in the forced convection case. Consequently, an improvement of 28% of the mass yield in forced convection is observed reflecting the major interest granted to forced convection in solar still.

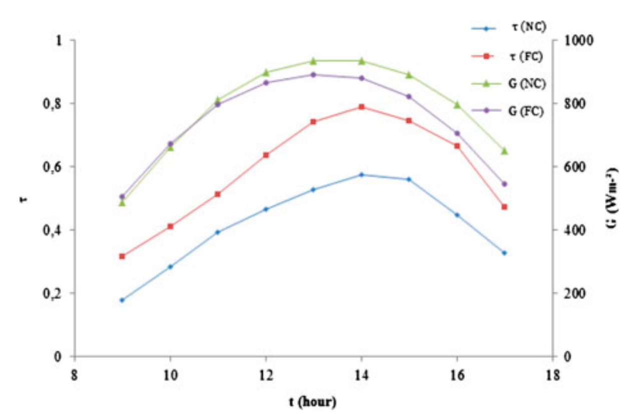

Fig. 9. Evolution of the mass yield and the solar flow during the day in natural and forced convection. (NC): (14 July 2013) $G_{\text{moy}} = 785.1$ W m^{-2}, $T_{\text{amb}} = 31$°C, $H_{\text{amb}} = 51\%$, $\dot{m}_a = 4.1$ kg h^{-1}. (FC): (04 July 2013) $G_{\text{moy}} = 784.1$ W m^{-2}, $T_{\text{amb}} = 32$°C, $H_{\text{amb}} = 48\%$, $\dot{m}_a = 4.1$ kg h^{-1}, $V = 3.34$ ms^{-1}.

4. Conclusion

In this work, an experimental device of an inclined solar film evaporator is performed. The evaporator is completed by a protocol of measures. It is submitted to real site exploitation conditions. The follow-up of its working is made during some days of summer 2013. The results of this study showed the existence of the two zones: a heating zone and an evaporation zone at the level of the liquid film falling on the inclined metal plane plate. A particular attention is paid to estimate the evaporated mass flow rate. An improvement of 43% in the evaporated mass flow rate in forced convection compared with the natural convection is calculated. Concerning the thermal and mass maxima yields of the solar evaporator, these two parameters are higher in forced convection than in natural convection. They exceed 80% under operating parameters of Bizerte region. This device can produce more than 21 L of evaporated water per day (for a surface of 2 m^2), in the case of the forced convection i.e. an improvement in production of 7 L in relation to the natural convection. These results prove that the device can be used to complete solar still. The next step will be devoted to connect the solar evaporator to a condenser to recover fresh water.

Nomenclature

b	—	width of the evaporator (m)
h	—	height of the evaporator (m)
H	—	relative humidity (%)
G	—	solar flux density (W m^{-2})
G_{moy}	—	average solar flux density (W m^{-2})
L	—	length of the evaporator (m)
L_v	—	latent heat of evaporation (J kg^{-1})
$\dot{m}_a$	—	mass flow rate of feed water (kg s^{-1})
$\dot{m}_{evp}$	—	evaporated mass flow rate (kg s^{-1})
m_s	—	mass of brine (kg)
$\dot{m}_s$	—	mass flow of brine (kg s^{-1})
t	—	time (h)
T	—	temperature (°C)
V	—	velocity of air aspiration (ms^{-1})
Greek symbols		
η	—	thermal yield
τ	—	mass yield
Subscripts		
amb	—	ambient
e	—	entering of the evaporator
s	—	outlet of the evaporator
Acronyms		
NC	—	natural convection
FC	—	forced convection
d	—	day

References

[1] M.T. Chaibi, An overview of solar desalination for domestic and agriculture water needs in remote arid areas, Desalination 127 (2000) 119–133.

[2] G.N. Tiwari, Y.P. Yadav, Comparative designs and long term performance of various designs of solar distiller, Energy Convers. Manage. 27 (1987) 327–333.

[3] K. Rajvanshi, Effect of various dyes on solar distillation, Sol. Energy 27 (1981) 51–65.

[4] B. Bouchekima, B. Grosb, R. Ouahes, M. Diboun, The performance of the capillary film solar still installed in South Algeria, Desalination 137 (2001) 31–38.

[5] A.Z. Al-Garni, Productivity enhancement of single slope solar still using immersion-type water heater and external cooling fan during summer, Desalin. Water Treat. 52 (2014) 6295–6303.

[6] A.K. Sethi, V.K. Dwivedi, Exergy analysis of double slope active solar still under forced circulation mode, Desalin. Water Treat. 51 (2013) 7394–7400.

[7] J. Orfi, M. Laplante, H. Marmouch, N. Galanis, B. Benhamou, S. Ben Nasrallah, C.T. Nguyen, Experimental and theoretical study of a humidification dehumidification water desalination system using solar energy, Desalination 168 (2004) 151–159.

[8] H. Marmouch, J. Orfi, S. Ben, Nasrallah, Effect of a cooling tower on a solar desalination system, Desalination 238 (2009) 281–289.

[9] A.H. El-Shazlya, M.M. El-Goharyb, M.E. Ossman, Performance characteristics of a solar humidification–dehumidification unit using packed bed of screens as the humidifier, Desalin. Water Treat. 16 (2010) 17–28.

[10] S. Ben Jabrallah, A.S. Cherif, B. Dhifaoui, A. Belghith, J.P. Corriou, Experimental study of the evaporation of a falling film in a closed cavity, Desalination 18 (2005) 197–206.

[11] S. Ben Jabrallah, A. Belghith, J.P. Corriou, Etude des transferts couplés de matière et de chaleur dans une cavité rectangulaire: application à une cellule de distillation (Study of coupled heat and mass transfer in a rectangular cavity: Application to a distillation cell), Int. J. Heat Mass Transfer 45 (2002) 891–904.

[12] W.M. Yan, Y.L. Tsay, T.F. Lin, Simultaneous heat and mass transfer in laminar mixed convection flows between vertical parallel plates with asymmetric heating, Int. J. Heat Mass Transfer 10 (1989) 217–237.

[13] S. Ben Jabrallah, A. Belguith, J.P. Corriou, Convective heat and mass transfer with evaporation of fallin film in cavity, Int. J. Therm. Sci. 45 (2006) 16–28.

[14] A.S. Cherif, S. Ben Jabrallah, J.P. Corriou, A. Belghith, Intensification of the liquid film evaporation in a vertical channel, Desalination 250 (2010) 433–437.

[15] Xingsen Mu, Shengqiang Shen, Yong Yang, Xiaohua Liu, Experimental study of falling film evaporation heat transfer coefficient on horizontal tube, Desalin. Water Treat. 50 (2012) 310–316.

[16] A. Nasr, C. Debbissi, S. Ben, Nasrallah, Numerical study of evaporation of liquid film by mixed convection in partially wetted vertical channel, Desalin. Water Treat. 46 (2012) 10–20.

[17] W.M. Yan, Mixed convection heat and mass transfer in a vertical channel with film evaporation, Can. J. Chem. Eng. 71 (1993) 54–62.
[18] T.R. Shembharkar, B.R. Pai, Prediction of film cooling with a liquid coolant, Int. J. Heat Mass Transfer 29 (1986) 899–899.
[19] R. Ben Radhia, S. Harmand, J.P. Corriou, S. Ben Jabrallah, Liquid film evaporation enhancement in a vertical annulus with preheated air flow, Desalin. Water Treat. 52 (2014) 1654–1661.
[20] Y.L. Tsay, T.F. Lin, W.M. Yan, Cooling of falling liquid film through interfacial heat and mass transfer, Int. J. Multiphase Flow 16 (1990) 61–71.
[21] J.H. Wang, N. Gao, Y. Deng, Y. Li, Solar power-driven humidification–dehumidification (HDH) process for desalination of brackish water, Desalination 305 (2012) 17–23.
[22] C. Khelif, B. Touati, Semi-empirical characterization of a greenhouse-effect cascades solar distiller, Renew. Energy 19 (2000) 103–110.